Solid State Communications 250 (2017) 104–107

Contents lists available at ScienceDirect

Solid State Communications

journal homepage: www.elsevier.com/locate/ssc

Communication

Massless Dirac fermions in semimetal HgCdTe

M. Marchewka*, J. Grendysa, D. Żak, G. Tomaka, P. Śliż, E.M. Sheregii

Centre for Microelectronics and Nanotechnology, University of Rzeszów, Pigonia 1, 35-959 Rzeszów, Poland

ARTICLE INFO

Keywords:
Topological surface states
3D strained HgCdTe system
Magnetotransport experiment

ABSTRACT

Magneto-transport results obtained for the strained 100 nm thick Hg_{1-x} Cd_xTe (x=0.135) layer grown by MBE on the CdTe/GaAs substrate are interpreted by the 8×8 kp model with the in-plane tensile strain. The dispersion relation for the investigated structure proves that the Dirac point is located in the gap caused by the strain. It is also shown that the fan of the Landau Levels (LL's) energy calculated for topological protected surface states for the studied HgCdTe alloy corresponds to the fan of the LL's calculated using the graphen-like Hamiltonian which gives excellent agreement with the experimental data for velocity on the Fermi level equal to $v_f \approx 0.85\times10^6$ m/s. That characterized strained Hg_{1-x} Cd_xTe layers ($0.13 < x < 0.14$) are a perfect Topological Insulator with good perspectives of further applications.

1. Introduction

In the last decade one of the most surprising discoveries at the intersection of the condensed matter physics and materials science is the realization that relativistic effects, strong for electrons in heavy elements (strong spin-orbital interaction) what lead to striking elementary excitations, such as Dirac, Majorana, and Weyl fermions in several classes of solids and nanostructures [1]. An interest phenomena have generated in new state of quantum matter - topological insulators (TI) - which behaves as an insulator in its interior and as a metal on it's boundaries [2–11]. The surface states of a three-dimensional (3D) TI such as 3D strained HgTe layers [9] Bi_2Se_3, Bi_2Te_3, and Sb_2Te_3 [12–15], consist of a single massless Dirac cone due to the crossing of two branches of bands at the surface. That are known as topologically protected surface states (TPSS) [13] - resistant against the time reversal invariant prturbation. Frequently, there are two edge states as cones belonging to the top and the bottom surfaces for the whole sample on which the transport of Dirac fermions is realized over the conductance with the Berry phase of π [16–19].

For the case of the 3D HgTe the uniaxial strain along (001) axis lifts the degeneracy of the Γ_8 bands by breaking the cubic symmetry at the Γ-point of the Brillouin zone (BZ) and opens an insulating gap which makes such systems as 3D TI: the tensile strain caused by the mismatch between the substrate - CdTe and HgTe lattice is enough to open a gap between $\Gamma_8^{3/2}$ and $\Gamma_8^{1/2}$ [9]. After that the TPSS are left inside the energy gap, what allows to received a truly insulating bulk system with the metallic phase at the surface.

In our previous work it was shown that analogous situation as for the pure HgTe, is realized in a strained layer of the semimetal Hg_{1-x} Cd_xTe alloys ($x < 0.16$ at T=4.2 K) [20]. The additional degree of freedom exists in the case of semimetal HgCdTe: possibility to change the energy dispersion of carriers using the composition as a parameter. The latter one enables to reach as close as possible to the so-called 3D Dirac point where the Γ_6 and Γ_8 are crossing in the BZ and a linear disperse in all directions around the critical point in the 3D momentum space takes place [21]. The key questions are: i) how it will affect to TPSS; ii) how it can influence the charges transport on the TPSS in case of high intrinsic electron density in the investigated samples [8,20]. These questions are really important for the realization of a Weyl semimetal phase based on the HgCdTe, e.g. in Hg_{1-x-y} Cd_xMn_yTe [22].

In this paper the experimental results on magnetotransport – Integer Quantum Hall Effect (IQHE) and Shubnikov-de Haas oscillations (SdH) – obtained for the strained 100 nm wide $Hg_{0.865}Cd_{0.135}$ Te layer (it still corresponds to a semi-metallic type of a band-structure but it is close to the 3D Dirac point) are interpreted on the basis of the 8×8 **kp** model. It will be shown that the fan of the Landau Levels (LL's) calculated by **kp** model for TPSS of the studied HgCdTe alloy corresponds to the fan of the LL's calculated using the graphen-like Hamiltonian which gives excellent agreement with experimental data for velocity on the Fermi level $v_f \approx 0.85\times10^6$ m/s what is important for future applications of this material as TI.

2. Numerical calculations

The **kp** model used an eight band description of the band structure including all second-order terms representing the remote-band con-

* Corresponding author.
E-mail address: marmi@ur.edu.pl (M. Marchewka).

http://dx.doi.org/10.1016/j.ssc.2016.11.020
Received 13 September 2016; Received in revised form 14 November 2016; Accepted 25 November 2016
Available online 27 November 2016

Table 1
Band structure parameters of HgTe and CdTe (according to Refs. [23,24]).

	HgTe	CdTe		HgTe	CdTe
E_g	−0.303 eV	1.606 eV	C	−3.83 eV	−4.06 eV
E_v	0	−570 meV	a	0	−0.7 eV
Δ	1.08 eV	0.91 eV	b	−1.5 eV	−1.17 eV
E_P	18.8 eV	18.8 eV	d	−2.08 eV	−3.2 eV
F	0	−0.09	C_{11}	53.6 GPa	53.6 GPa
γ_1	4.1	1.47	C_{12}	36.6 GPa	37.0 GPa
γ_2	0.5	−0.28	C_{44}	21.2 GPa	19.9 GPa
γ_3	1.3	0.03			
κ	−0.4	−1.31			

tributions with the first-order terms attributed to the $\Gamma_8^{3/2}$ - heavy hole, $\Gamma_8^{1/2}$ - light hole bands, and the $\Gamma_6^{1/2}$ - conduction band as well as $\Gamma_7^{1/2}$ - cleaved by the spin-orbital interaction [23,24]. The available band-structure parameters used in the eight band description, are presented in Table 1. The detailed descriptions of the calculation and the results for the mixed Hg_{1-x} Cd_xTe 3D TI for the different widith of the layers and different tensile strain are presented in Ref. [25]. The calculations of the energy spectrum are provided in the framework of the envelope function approach (EFA) where z - axis coincides with the growth direction of the 3D system. The finite difference method (FDM) with the common central difference form is particularly employed in the discretization procedure.

The results of the calculations are presented in Figs. 1a)–d). For the strained 75 nm thick HgTe layer (Fig. 1a) the dispersion relations calculated by the above mentioned method look the same as those ones in the work [9]. The exposed TPSS appear here in the gap induced by the strain as a small upper part of the Dirac cones which are formed inside of the $\Gamma_8^{3/2}$ band.

Similar like in the Ref. [9] (supp. material) and in the [26] the dispersion relation as well as the charge distribution for investigated material were detailed analysis in Ref. [25]. It was shown that in the case of the mixed 3D HgCdTe TI the shape of the $|\Psi(z)|^2$ in the mini gap region (where the linear dispersion relation is presented) fulfills the definition of edge states [26] for this materials.

The band-structure calculations within the eight-band **kp** model for different values of x ($0.135 < x < 0.15$) and at T=4.2 K with the 100 nm thick strained layers shows also that the Dirac point can be visible in the strained gap (Figs. 1b, c).

The numerical calculations performed for $Hg_{0.865}Cd_{0.135}$ Te (Fig. 1b) show that the smaller inverted energy gap together with the unaxial tensile strain along (001) direction (for 100 nm thick layers) make the Dirac point for TPSS located a little bit above the top of the $\Gamma_8^{3/2}$ band. Beside that the gap between $\Gamma_8^{3/2}$ and $\Gamma_8^{1/2}$ which is induced by the strain is greater than for the pure 3D HgTe TI and is equal to about 30 meV for x=0.135 at the Γ point of BZ (though the mismatch is reduced by≈13% but the effect of the tensile is much greater due to the energy dispersion closed to the linear one in a bulk part of a sample).

The position of the Dirac point goes up together with the increase of the x-value. For x=0.135 it is located around −10 meV (Fig. 1b)), and it practically touches the top of the band (with a small gap about 0.5 meV). For the higher values of x the Dirac point is being created inside the strained gap, for x=0.145 it is located about 7 meV above $\Gamma_8^{3/2}$ - Fig. 1c). It is necessary to underline that the position of the Dirac point in the energy scale is responsible for the shape of the energy dispersion for the TPSS: it can be expected that the linear dispersion law is applicable to a wider range of E(k) for the case when x-value is close to 0.15.

A different situation takes place in the same temperature for the Hg_{1-x} Cd_xTe layers with the $x \geq 0.150$. For $x = 0.155$ the Dirac point at surfaces is violated: a gap of about 4 meV between the upper and the lower part of the Dirac cone appears (see inset Fig. 1d) and then these states do not represent the TPSS anymore.

3. Results

The results of the IQHE for the strained 100 nm wide $Hg_{0.865}$ Cd $_{0.135}$

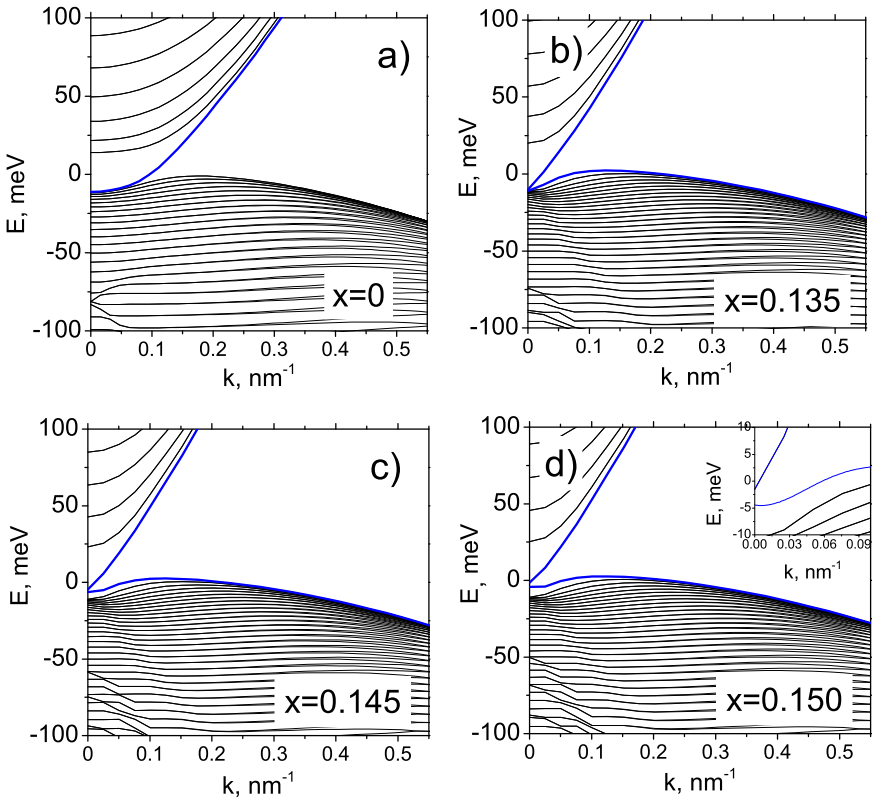

Fig. 1. Dispersion relation for 100 nm wide strained 3D Hg_{1-x} Cd_xTe layers with: a) x=0, b) x=0.135, c) x=0.145 and d) x=0.150. A blue line present the TPSS.

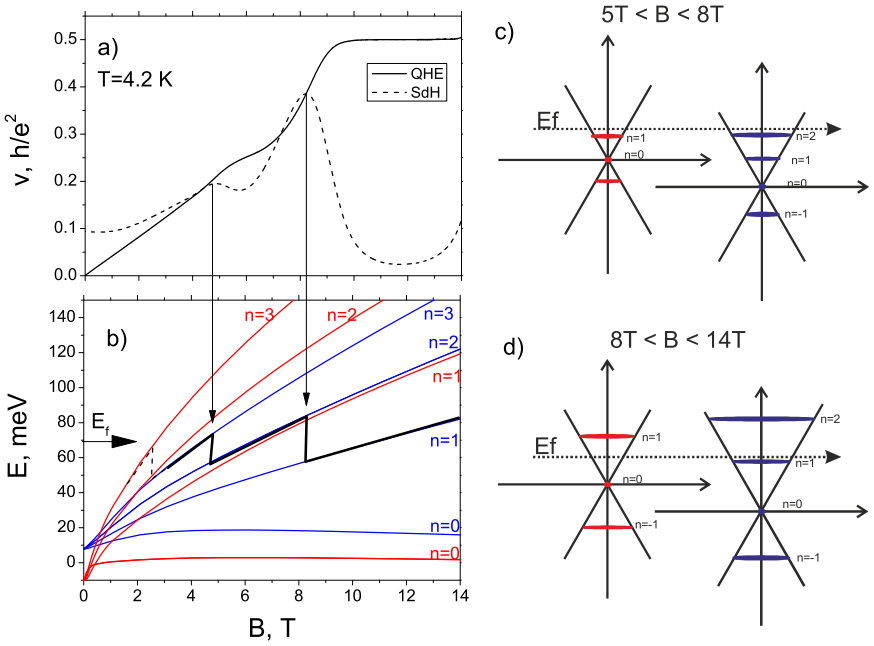

Fig. 2. a) The SdH oscillations and the IQHE for 4.2 K for 100 nm wide $Hg_{0.865}Cd_{0.135}$ Te and b) the LL's fan calculated for two Dirac cones for two interfaces; c) and d) represent the LL's under the magnetic field region between 5 and 8 T and 8 and 14 T respectively.

Te layer obtained at 4.2 K are presented in Fig. 2a). The even filling factor ν of 2, 4 and 6 means that two independent surfaces should be taken into account in the fermion transport - on the top and the bottom of a sample - its corresponds two Dirac cones model. As it is shown in Fig. 2c) and d) in order to get the filling factor $\nu = 2$ it is necessary to have the Landau index N_b=1 (the bottom surface) and $N_t = 2$ for the top surface.

The LL's presented in Fig. 2 were calculated from the above mentioned eight band **kp** model but the experimental data can also be fitted by the LL's fan energy obtained from graphene-like Hamiltonian. In order to obtain a good agreement with the graphene-like LL's energies and experimental curves of R_{xy} and R_{xx} the difference between the positions of the Dirac points for two surfaces should by equal to about 20 meV. As it is shown in Figs. 2c,d it is worth to mention that the LL's fan calculated by the 8×8 **kp** model with band-structure parameters presented in Table 1, are in excellent agreement with the one obtained using the graphene-like Hamiltonian if the Fermi level velocity is equal to about 0.85×10^6 m/s.

The same calculations performed for pure HgTe (x=0) lead to the Fermi level velocity v_f=0.43×10^6 m/s what confirms the result obtained by the authors of Ref. [9] ($\hbar v_f$ =280 meV nm).

The Fermi velocity can be directly received from $E(k)$ relations $\Delta E = \hbar v_f \Delta k$ (in the linear region of the dispersion relation) that are shown in Fig. 1. For the $Hg_{0.865}Cd_{0.135}$ Te strained layers the velocity of the fermions for the TPSS obtained by this way is equal to 0.85×10^6 m/s also.

Such velocity allows to observe the quantized Hall conductance on TPSS even without external gate voltage and on the background of the bulk states. It is interesting to remark that the TPSS are visible in magneto-transport for the wide range of the gate voltage applied into the pure HgTe 3D 70-nm-thick sample due to their remarkable screening properties according to Ref. [26]. This hypothesis could be applied to our $Hg_{0.865}Cd_{0.135}$ Te sample also due to high electron density. Besides, the high temperature stability of the observed TPSS was shown in Ref. [20].

4. Summary

To sum up briefly, it is shown that the LL's fan calculated for TPSS for the studied HgCdTe alloy using the eight band kp model corresponds to the one calculated by graphene Hamiltonian and characterized by $v_f \approx 0.85\times10^6$ m/s what is in excellent agreement with the experimental IQHE- and SdH-curves. On the other hand, this value of the Fermi velocity is two times greater than for the strained HgTe TI Ref. [9] and for other kind of TI - approximately 5×10^5 m/s, for Bi_2Se_3 [12], or 3.4×10^5 m/s for the same compound according to Ref. [27].

Thus, the strained 3D $Hg_{0.865}Cd_{0.135}$ Te is a Topological Insulator with high value of the Fermi velocity (close to the Fermi velocity value for graphene) which is a significant advantage. The last one concerns although the HgCdTe based quantum wells near the phase transition between the semi-metal and semiconductor [28]. Besides, the bigger strained energy gap inside the sample than in the case of strained HgTe, and a higher position of the Dirac points on the energy scale lead to an increase in the attractiveness of the Topological Insulators based on semimetal HgCdTe alloy for future applications. All these advantages follow from significantly lower value of the electron momentum on the Fermi level in comparison with pure HgTe and the energy dispersion is closer to linearity in the wider energy range.

Acknowledgements

We acknowledge support from the authorities of the Podkarpackie Voiwodership (Marshals Office of the Podkarpackie Voivodship of Poland), contract WND-PPK.01.03.00-18- 053/12.

References

[1] L. Balent, Physics 4 (2011) 36.
[2] C.L. Kane, E.J. Mele, Phys. Rev. Lett. 95 (2005) 226801.
[3] B.A. Bernevig, Shou-Cheng Zhang, Phys. Rev. Lett. 96 (2006) 106802.
[4] B. Andrei Bernevig, Taylor L. Hughes, Shou-Cheng Zhang, Science 314 (2006) 1757.
[5] M. König, S. Wiedmann, C. Brne, A. Roth, H. Buhmann, L.W. Molenkamp, Xiao-Liang Qi, Shou-Cheng Zhang, Science 318 (2007) 5851.
[6] Liang Fu, C.L. Kane, E.J. Mele, Phys. Rev. Lett. 98 (2007) 106803.
[7] Liang Fu, C.L. Kane, Phys. Rev. B 76 (2007) 045302.
[8] D. Hsieh, D. Qian, L. Wray, Y. Xia, Y.S. Hor, R.J. Cava, M.Z. Hasan, Nature 452 (2008) 970–974.
[9] C. Brüne, C.X. Liu, E.G. Novik, E.M. Hankiewicz, H. Buhmann, Y.L. Chen, X.L. Qi, Z.X. Shen, S.C. Zhang, L.W. Molenkamp, Phys. Rev. Lett. 106 (2011) 126803.
[10] M.Z. Hasan, C.L. Kane, Rev. Mod. Phys. 82 (2010) 3045.
[11] Xiao-Liang Qi, Shou-Cheng Zhang, Rev. Mod. Phys. 83 (2011) 1057.

[12] Y. Xia, D. Qian, D. Hsieh, L. Wray, A. Pal, H. Lin, A. Bansil, D. Grauer, Y.S. Hor, R.J. Cava, M.Z. Hasan, Nature Physics 5 (2009) 398–402.
[13] Haijun Zhang, Chao-Xing Liu, Xiao-Liang Qi, Xi Dai, Zhong Fang, Shou-Cheng Zhang, Nature Physics 5 (2009) 438–442.
[14] Y.L. Chen, J.G. Analytis, J.H. Chu, Z.K. Liu, S.K. Mo, X.L. Qi, H.J. Zhang, D.H. Lu, X. Dai, Z. Fang, S.-C. Zhang, I.R. Fisher, Z. Hussain, Z.X. Shen, Science 325 (2009) 178.
[15] D.X. Qu, Y.S. Hor, J. Xiong, R.J. Cava, N.P. Ong, Science 329 (2010) 821.
[16] M. Berry, Nature Physics 6 (2010) 148150.
[17] L.B. Zhang, Kai Chang, X.C. Xie, H. Buhmann, L.W. Molenkamp, New J. Phys. 12 (2010) 083058.
[18] Z.Z. Zhang, Kai Chang, F.M. Peeters, Phys. Rev. B 77 (2008) 235411.
[19] Kai Chang, Wen-Kai Lou, Phys. Rev. Lett. 106 (2011) 206802.
[20] G. Tomaka, J. Grendysa, P. Śliż, C.R. Becker, J. Polit, R. Wojnarowska, A. Stadler, E.M. Sheregii, Phys. Rev. B 93 (2016) 205419.
[21] S.M. Young, S. Zaheer, J.C.Y. Teo, C.L. Kane, E.J. Mele, A.M. Rappe, Phys. Rev. Lett. 108 (2012) 140405.
[22] Daniel Bulmash, Chao-Xing Liu, Xiao-Liang Qi, Phys. Rev. B 89 (2014) 081106 (R).
[23] E.G. Novik, A. Pfeuffer-Jeschke, T. Jungwirth, V. Latussek, C.R. Becker, G. Landwehr, H. Buhmann, L.W. Molenkamp, Phys. Rev. B 72 (2005) 035321.
[24] A. Pfeuffer-Jeschke, Ph.D. thesis, Physikalisches Institut, Universitt Würzburg, Germany, 2000.
[25] M. Marchewka, Physica E 84 (2016) 407–414.
[26] C. Brüne, C. Thienel, M. Stuiber, J. Böttcher, H. Buhmann, E.G. Novik, Chao-Xing Liu, E.M. Hankiewicz, L.W. Molenkamp, Phys. Rev. X 4 (2014) 041045.
[27] Peng Cheng, Canli Song, Tong Zhang, Yanyi Zhang, Yilin Wang, Jin-Feng Jia, Jing Wang, Yayu Wang, Bang-Fen Zhu, Xi Chen, Xucun Ma, Ke He, Lili Wang, Xi Dai, Zhong Fang, Xincheng Xie, Xiao-Liang Qi, Chao-Xing Liu, Shou-Cheng Zhang, Qi-Kun Xue, Phys. Rev. Lett. 105 (2010) 076801.
[28] Wen Yang, Kai Zhang, Shou-Cheng Chang, Phys. Rev. Lett. 100 (2008) 056602.